

# Practical and highly sensitive elemental analysis for aqueous samples containing metal impurities employing electrodeposition on indium-tin oxide film samples and laser-induced shock wave plasma in low-pressure helium gas

KOO HENDRIK KURNIAWAN,<sup>1,\*</sup> MARINCAN PARDEDE,<sup>2</sup> RINDA HEDWIG,<sup>3</sup> SYAHRUN NUR ABDULMADJID,<sup>4</sup> KURNIA LAHNA,<sup>4</sup> NASRULLAH IDRIS,<sup>4</sup> ERIC JOBILIONG,<sup>5</sup> HERY SUYANTO,<sup>6</sup> MARIA MARGARETHA SULIYANTI,<sup>7</sup> MAY ON TJIA,<sup>1,8</sup> TJUNG JIE LIE,<sup>1</sup> ZENER SUKRA LIE,<sup>1</sup> DAVY PUTRA KURNIAWAN,<sup>1</sup> AND KIICHIRO KAGAWA<sup>1,9</sup>

<sup>1</sup>Research Center of Maju Makmur Mandiri Foundation, 40/80 Srengseng Raya, Jakarta 11630, Indonesia

<sup>2</sup>Department of Electrical Engineering, University of Pelita Harapan, 1100 M.H. Thamrin Boulevard, Lippo Village, Tangerang 15811, Indonesia

<sup>3</sup>Department of Computer Engineering, Bina Nusantara University, 9 K.H. Syahdan, Jakarta 14810, Indonesia

<sup>4</sup>Department of Physics, Faculty of Mathematics and Natural Sciences, Syiah Kuala University, Darussalam, Banda Aceh 23111, NAD, Indonesia

<sup>5</sup>Department of Industrial Engineering, University of Pelita Harapan, 1100 M.H. Thamrin Boulevard, Lippo Village, Tangerang 15811, Indonesia

<sup>6</sup>Department of Physics, Faculty of Mathematics and Natural Sciences, Udayana University, Kampus Bukit Jimbaran, Denpasar 80361, Bali, Indonesia

<sup>7</sup>Research Center for Physics, Indonesia Institute of Sciences, Kawasan PUSPIPTEK, Serpong, Tangerang Selatan 15314, Banten, Indonesia

<sup>8</sup>Physics of Magnetism and Photonics Group, Faculty of Mathematics and Natural Sciences, Bandung Institute of Technology, 10 Ganesha, Bandung 40132, Indonesia

<sup>9</sup>Fukui Science Education Academy, Takagi Chuou 2 choume, Fukui 910-0804, Japan

\*Corresponding author: [kurnia18@cbn.net.id](mailto:kurnia18@cbn.net.id)

Received 19 May 2015; revised 4 August 2015; accepted 4 August 2015; posted 5 August 2015 (Doc. ID 241214); published 26 August 2015

We have conducted an experimental study exploring the possible application of laser-induced breakdown spectroscopy (LIBS) for practical and highly sensitive detection of metal impurities in water. The spectrochemical measurements were carried out by means of a 355 nm Nd-YAG laser within N<sub>2</sub> and He gas at atmospheric pressures as high as 2 kPa. The aqueous samples were prepared as thin films deposited on indium-tin oxide (ITO) glass by an electrolysis process. The resulting emission spectra suggest that concentrations at parts per billion levels may be achieved for a variety of metal impurities, and it is hence potentially feasible for rapid inspection of water quality in the semiconductor and pharmaceutical industries, as well as for cooling water inspection for possible leakage of radioactivity in nuclear power plants. In view of its relative simplicity, this LIBS equipment offers a practical and less costly alternative to the standard use of inductively coupled plasma-mass spectrometry (ICP-MS) for water samples, and its further potential for *in situ* and mobile applications. ©2015 Optical Society of America

**OCIS codes:** (140.3440) Laser-induced breakdown; (020.0020) Atomic and molecular physics.

<http://dx.doi.org/10.1364/AO.54.007592>

## 1. INTRODUCTION

It is well known that highly sensitive and accurate spectrochemical analysis is widely required for the inspection and assessment of industrial products and industrial wastes as well as for process control in various industries. Along with the commonly adopted standard techniques for trace element analysis, such as ICP-MS, ICP-OES, AAS, and XRF spectrometries, laser-induced breakdown spectroscopy (LIBS) has become a new alternative for practical and rapid spectrochemical analysis. This technique,

owing to its continued improvement and extension, has become one of the most widely adopted spectrochemical techniques employed in various fields of application [1–5]. Recently, with the employment of low-pressure ambient gas, the resulting spectral resolution and detection sensitivity have been greatly enhanced, approaching those of the standard techniques for trace element analysis. This was demonstrated by the successful detection and quantitative analysis of H and D in a Zircaloy tube, which have eluded detection by conventional LIBS [6].

The world is currently facing the serious problems of increasing need for quality water for daily human life in view of the fast growing world population, and increasing water pollution arising from poorly handled industrial and human wastes. In the meantime, the rapid expansion of industry is taking place in wide ranging areas, such as the production and development of semiconductor-based microelectronic, optoelectronic, and photonic devices, as well as the pharmaceutical industry. These industries are also crucially in need of high purity water supplies. No less important is the problem faced by the continued proliferation of nuclear power plants to meet the pressing demand of an alternative energy source that is sustainable, clean, and efficient. The stringent safety measures imposed on their operation requires the strict implementation of timely and regular inspection for possible leakage of radioactivity. This is commonly carried out among other techniques, by the detection of radioactive fission products such as Sr and Cs in the cooling water. The limit of detection (LOD) for the unwanted elements in those cases is generally well below the parts per million (ppm) level. For instance, it is below 100 parts per billion (ppb) for life-endangering heavy metals in the polluted water and sub-ppm in the high-purity water used in semiconductor manufacturing processes [7]. For those purposes, the samples are usually brought to laboratories where sensitive spectrochemical equipment such as ICP-MS, ICP-OES, AAS, or XRF spectrometers are available. However, the need for sample transportation and special sample treatment or measurement preparation have made them highly unwieldy as well as relatively costly operations for frequent and regular inspections. A more practical *in situ* operated and less expensive but equally sensitive technique is clearly desirable.

As mentioned earlier, LIBS operated with low-pressure ambient gas may offer the most promising solution. Recently, the detection of trace metal elements in water was reported using LIBS in combination with electrodynamic balance (EDB) technology [8]. While an impressive LOD of less than 100 ppb was reported, the method is perhaps too sophisticated to qualify as the practical alternative mentioned above. On the other hand, a similar range of LOD was previously achieved by means of LIBS operated at low-pressure ambient air with the water samples of metal impurities electrodeposited on a metal (nickel to be specific) plate, which serves simultaneously as an impurity collecting electrode and a hard subtarget for the generation of strong plasma. Unfortunately, the result was not sufficiently reproducible as the deposited impurity film easily fell off from the metal electrode during laser shots. In addition, the use of a metal subtarget may interfere with the detected emission spectrum of the trace element in question and thereby impair detection accuracy and sensitivity [9].

In this study, the metal electrode is replaced by a thin indium-tin oxide (ITO) glass for electrodeposition of the trace metallic elements from the water sample, and to serve as the subtarget. In addition, the plasmas are generated in this experiment by employing the third harmonic (355 nm) instead of the fundamental wavelength of a Nd-YAG laser. Further, taking note of the important effect of ambient gas pressure on emission spectra quality, different gases of  $N_2$  and He at atmospheric and low pressure are employed in this experiment for

comparison and exploration of the most favorable ambient gas condition.

## 2. EXPERIMENTAL PROCEDURE

A complete schematic diagram of the experimental arrangement is similar to that in our previous works [6,9]. It is modified only by the change in laser source. The laser used in this experiment is a 355 nm Nd-YAG (Quanta Ray, INDI SERIES, 125 mJ, 5 ns) operated in Q-switched mode at a 10 Hz repetition rate. The choice of laser source is made as it is found more effective than infrared radiation in releasing the metal elements from the deposited film samples and, hence, more effective for the ablation process [10]. The laser output energy is fixed at approximately 40 mJ by means of a set of filters. The laser beam is directed to the sample with a lens of focal length  $f = 120$  mm and a quartz window. The irradiation is carried out by positioning the lens at a distance of 115 mm from the sample surface ( $-5$  mm defocused position). This results in an enlarged irradiated spot of approximately 0.3 mm diameter and an increased amount of ablated impurity elements with minimal damage to the ITO glass substrate.

Electrodeposition of metal elements contained in water was conducted by using an ITO glass of 20 mm  $\times$  20 mm  $\times$  1 mm as the collecting electrode in the setup described in Fig. 1. This and its counterelectrode were fixed in a parallel configuration with a separation of 50 mm in a 1000 ml beaker containing the water sample to be investigated. A DC voltage difference of 10–20 V was applied between the electrodes. A resistor of suitable resistance is inserted in the circuit to attain a uniform film with a desirable deposition time. During the electrodeposition process, water in the beaker was constantly stirred by means of a magnetic stirrer operated at a frequency of around 5 cycles per second. The duration of electrolysis was generally set for about 20 min, yielding a uniform/smooth thin film of around 100  $\mu$ m on the ITO substrate. The deposited films were subsequently dried at 80°C in vacuum ( $N_2$  gas at pressure of 260 Pa) for 20 min. The resulting films are found to be quite firmly attached to the ITO surface and thus overcome the problem with the metal substrate mentioned earlier [9].

In each experiment, the sample was rotated at 1 rpm to ensure that each laser pulse was directed onto a new sample position. The sample itself was placed in a small vacuum tight metal chamber measuring 11 cm  $\times$  11 cm  $\times$  12.5 cm, which was evacuated using a vacuum pump prior to being filled with  $N_2$  or He gas to the desired pressure. The gas pressure was thereafter maintained by a certain flow rate, which was regulated by a needle valve in the air line and a second valve in the pumping line. The chamber pressure was monitored by means of a digital Pirani gauge.

Spectral measurement of the secondary plasma emission was carried out by employing an optical multichannel analyzer (OMA system, Andor I\*Star intensified CCD 1024  $\times$  256 pixels) of 0.012 nm spectral resolution at 500 nm. This system was attached on one side to a spectrograph (McPherson Model 2061 with 1000 mm focal length  $f/8.6$  Czerny Turner configuration), which is connected to an optical fiber on the other end.

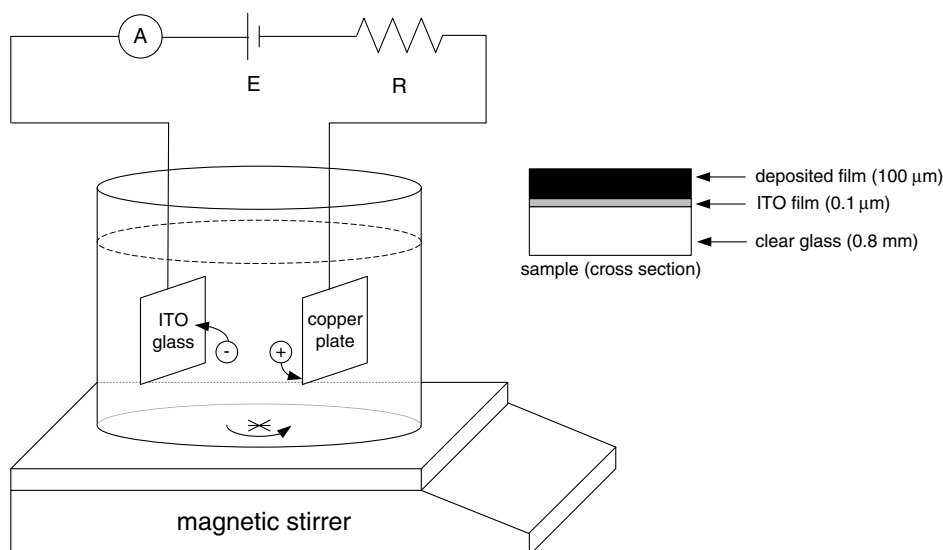


Fig. 1. Schematic setup of electrodeposition process.

### 3. RESULTS AND DISCUSSION

In our first experiment, an Hg film is deposited from a Hg standard solution of 1000 ppm Hg concentration, which is diluted to 1 ppm concentration by Hg-free tap water. Figure 2 shows the resulting plasma in  $N_2$  gas at a pressure of 260 Pa. This exhibits a hemispherical shape and shares basically the same features as those observed previously for shock wave plasma using other lasers and various surrounding gases. Specifically, it is seen to consist of two distinct parts, typical of shock-wave-induced plasma. Right in front of the target surface is a tiny primary plasma of very dense white. The other part is a much larger secondary plasma growing out of the primary plasma, extending far beyond it and displaying a multilayer

color structure associated with the In I 451.1 nm and In I 410.1 nm emission lines giving rise to the green yellowish color, and the H I 656.2 nm emission responsible for the red color. The radius of the secondary plasma is further found to increase with decreasing pressure of the surrounding gas, resulting in a vague plasma boundary when the  $N_2$  gas pressure is reduced below 50 Pa. The inset in this figure is a typical photo display of the deposited sample film with a crater created on it by a single laser shot. The randomly distributed dark spots over the film surface in this case indicate the deposited Hg metal particles, while the large roughly circular gray area is the ablated area on the ITO glass surface. In view of the large number of spots covered in the circle, it is reasonable to suppose that each ablated area contains more or less the same amount of ablated Hg particles.

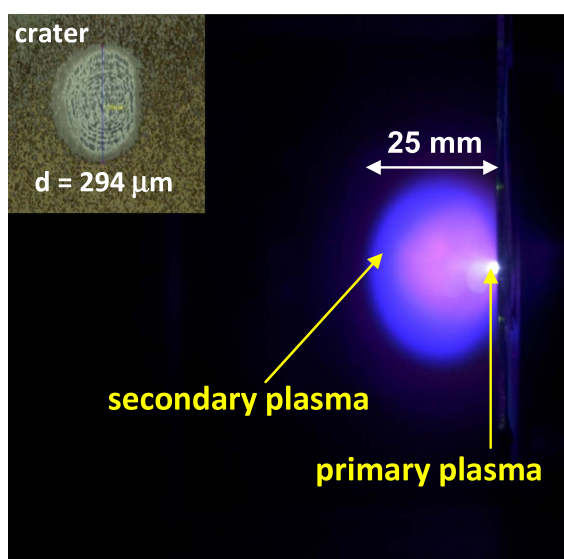
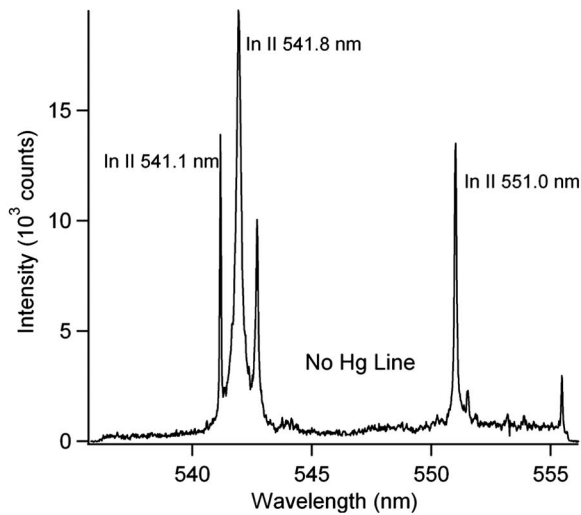
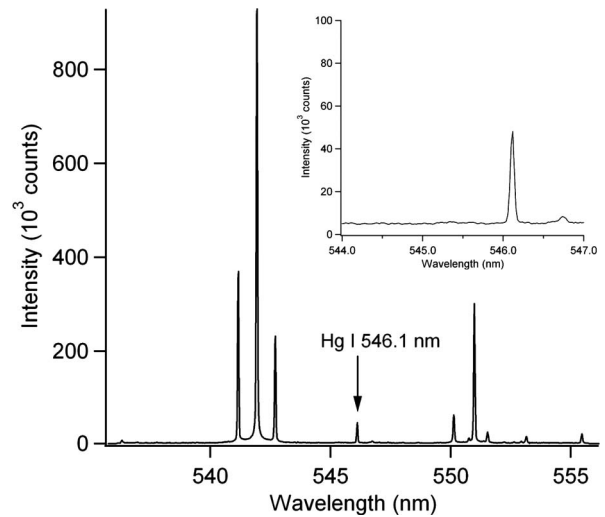


Fig. 2. Photograph of the plasma taken in  $N_2$  gas at 260 Pa using a 40 mJ 355 nm Nd-YAG laser. The inset in this figure is a photo display recorded by a high-resolution digital microscope camera of the deposited sample film with a crater created on it by a single laser shot.

Given the clear color signals of In and H emission lines in Fig. 2, it is noticeable that the contribution of the green Hg emission is missing in the color photo in the figure. Although this is likely due to the very low concentration (1 ppm) of Hg in the film, it remains desirable to further verify this observation of the photo by examining the associated emission spectrum. The measured spectrum presented in Fig. 3 (measured in  $N_2$  gas at atmospheric pressure) clearly confirms the absence of Hg emission around 546.0 nm, while the strong In emission lines from the ITO film are clearly observed and nicely correlate with the plasma colors displayed in Fig. 2. It should be pointed out that no ablation process takes place on the glass substrate since no Si emission is found in the observed wavelength region, as the laser irradiation is deliberately carried out under the defocused condition of  $-5$  mm to prevent the penetration of the laser beam into the glass substrate. Similar results are obtained when the  $N_2$  gas at atmospheric pressure is replaced with He surrounding gas at the same pressure. This may be explained by relatively weak bonding between the Hg impurity and the ITO surface. As a result, the Hg atoms are expected to be more readily ablated than the In atoms, and move faster ahead of the shock wave, which



**Fig. 3.** Emission spectra of Hg film taken in  $N_2$  gas at atmospheric pressure (98.8 kPa) using a 40 mJ 355 nm Nd-YAG laser.



**Fig. 4.** Emission spectra of Hg film taken in He gas at 2 kPa using a 40 mJ 355 nm Nd-YAG laser. The inset in this figure is the close-up view of the spectral region around the Hg emission line.

is mainly created by the In atoms. As they move faster than the shock wave front, the Hg atoms will have little chance to be thermally excited by the shock wave since the hottest region of the plasma is located just behind the shock wave front. The absence of the impurity emission line is amply confirmed by repeating the same measurement on the electrodeposited film samples of other impurity elements, such as Cu, Ag, Pb, Al, Li, and B. We are therefore led to conclude that the standard or commonly adopted LIBS using the suggested sample deposition technique is inadequate for the stated aim of this study.

This problem is somewhat similar to the so-called time mismatch between the passage of the ablated analyte element and the formation of the shock wave produced by the simultaneously irradiated and much more abundant host elements from the target (or subtarget in this case). This problem was first encountered in H analysis using conventional LIBS with a nanosecond Nd-YAG laser operating at its fundamental wavelength. The problem was then overcome by replacing the  $N_2$  gas at atmospheric pressure with low-pressure  $N_2$  gas. The formation of a shock wave in low-pressure  $N_2$  gas is known to be somewhat faster, and thereby improves the chance for exciting the fast-moving ablated element [6].

In the following experiment, a measurement was performed on the same sample using the same experimental setup, except for the separate replacement of the  $N_2$  gas at atmospheric pressure by  $N_2$  gas at low pressure (260 Pa) and He gas at low pressure (2 kPa). However, the result in only the case of low-pressure He gas is presented in Fig. 4 since the spectrum obtained in this case is much better. One observes in this figure a clear Hg I 546.0 nm emission along with the In emission lines. It is important to stress that the background in the vicinity of the Hg emission is actually very low compared to the signal intensity, as shown in the inset of Fig. 4. Background equivalent concentration (BEC) in this case is estimated to be less than 10 ppb, which is much lower than the ppm BEC in commonly cited LIBS standards [1–5,7,8]. The detection limit

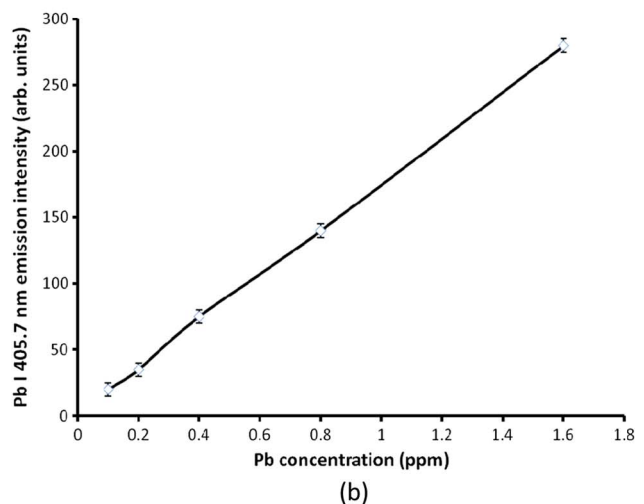
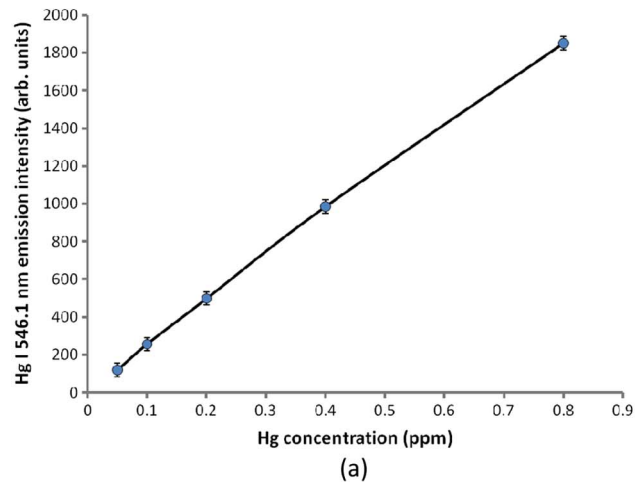


**Fig. 5.** Calibration lines of (a) Hg I 546.1 nm and (b) Pb I 405.7 nm.

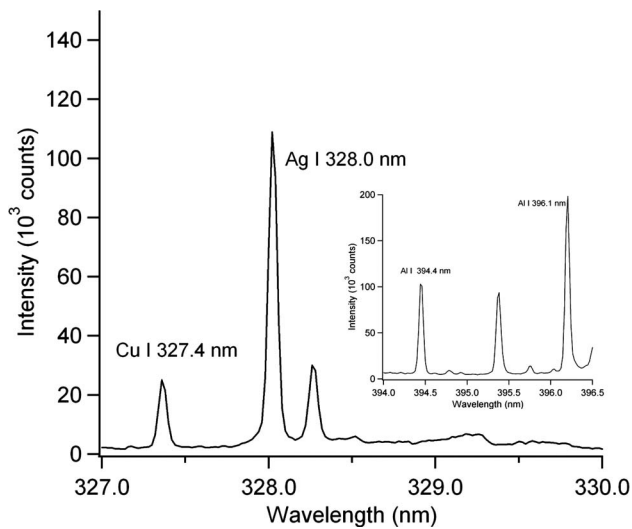


**Fig. 6.** Emission spectra of Ag I 328.0 nm and Cu I 327.4 nm in He gas at 2 kPa using a 40 mJ 355 nm Nd-YAG laser. The inset in this figure is the spectra of the Al I 394.4 nm and Al I 396.1 nm emission lines measured separately from the same film sample.

of this measurement is estimated to be as low as 4 ppb. The same result was also found for Pb, with an estimated detection limit of around 10 ppb. Further, for the possible application for quantitative analysis of these two elements, a series of aqueous samples containing those two metal impurities are prepared with a number of predetermined concentrations. The resulting emission intensity variations with respect to each impurity concentration are plotted in Fig. 5. The calibration curves clearly show a linear relationship featuring a large slope, implying sensitive intensity variations with respect to changes of the corresponding impurity concentrations. The curves are also seen to show extrapolated zero intercept.

The interesting and unusual results are further demonstrated in the following two important cases of application.

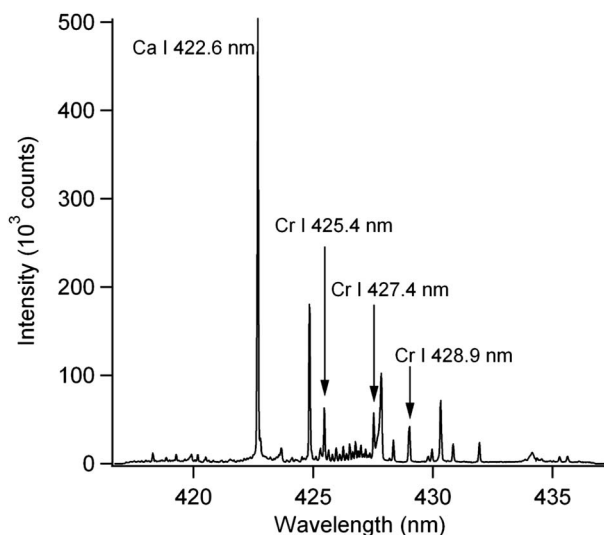


**Fig. 7.** Emission spectrum of Cr emission measured in He gas at 2 kPa using a 40 mJ 355 nm Nd-YAG laser.

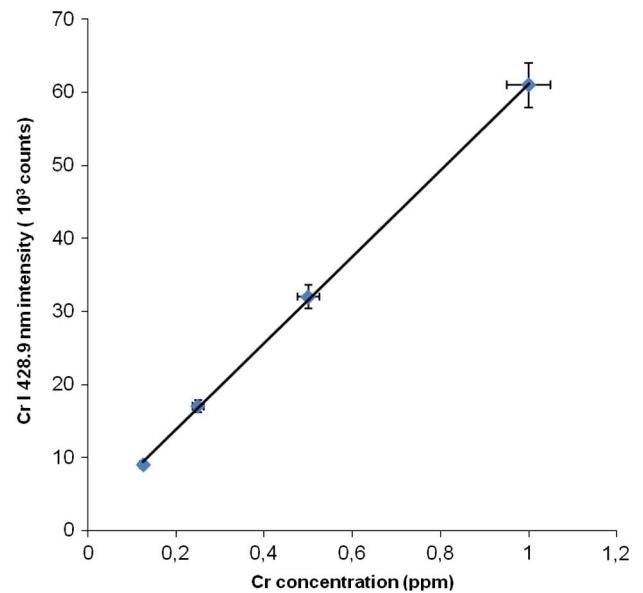


**Fig. 8.** Calibration line of Cr I 428.9 nm.

The first is concerned with the need for clean water for semiconductor manufacturing processes. The sample used for the experiment is a liquid containing trace metals of Al, Ag, Cu, and Cr, each with a concentration of 1 ppm, which is deposited on an ITO substrate by an electrolysis process. The resulting spectra are presented in Fig. 6 for the strong emission lines of Ag I 328.0 nm and Cu I 327.4 nm, which are seen to have extremely low background. Even stronger Al I 394.4 nm and Al I 396.1 nm emission lines are shown in the inset of Fig. 6. The detectable concentrations estimated from this spectra are 3 ppb for Ag, 10 ppb for Cu, and 3 ppb for Al. Presented in Fig. 7 is the Cr emission spectra consisting of the Cr I 425.4 nm, Cr I 427.4 nm, and Cr I 428.9 nm emission lines. The calibration curve of Cr is presented in Fig. 8, which shows

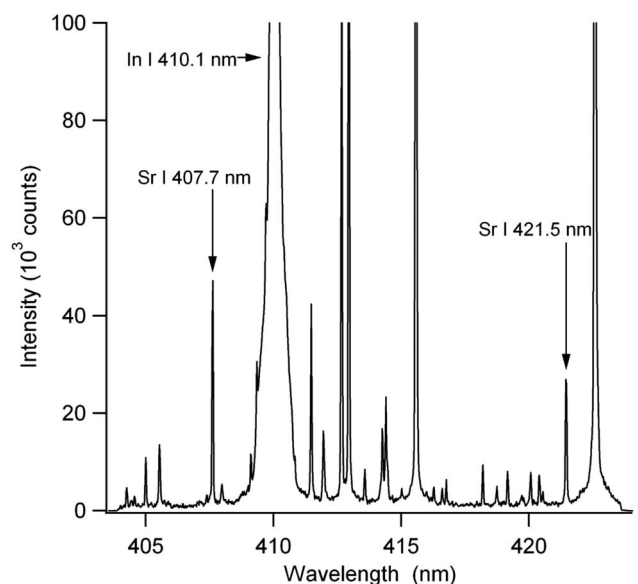


**Fig. 9.** Emission spectra of Sr I 407.7 nm and Sr I 421.5 nm in He gas at 2 kPa using a 40 mJ 355 nm Nd-YAG laser.

a linear relationship between Cr I 425.4 nm emission intensity and Cr concentration, with extrapolated zero intercept. The detectable concentration of Cr is estimated to be around 80 ppb.

The second case is related to the need for inspection of the cooling water in a nuclear power station. The samples are prepared with water containing 1 ppm of Sr. The resulting emission spectrum is shown in Fig. 9, from which the lowest detectable concentration is estimated to be 20 ppb, which is much lower than the maximum impurity levels tolerated in a nuclear power station.

#### 4. CONCLUSIONS

We have shown that use of the electrodeposition process for aqueous samples and the LIBS technique employing third-harmonic Nd-YAG laser pulses in low-pressure He gas have demonstrated the ability to detect and analyze a variety of metallic impurities in water with remarkably low concentrations. While the lowest impurity detectable in this experiment is in need of further data substantiation for the determination of the corresponding limits of detection, the current results nevertheless suggest the promising attainment of LOD comparable with that offered by ICP-MS, which is the currently adopted standard. In view of its simplicity, this spectrochemical equipment promises applications for regular and rapid, as well as relatively inexpensive and highly sensitive, detection and analysis.

#### REFERENCES

1. D. Winefordner, I. B. Gornushkin, T. Corell, E. Gibb, B. W. Smith, and N. Omenetto, "Comparing several atomic spectrometric methods to the super stars; special emphasis on laser induced breakdown spectrometry, LIBS, a future super star," *J. Anal. At. Spectrom.* **19**, 1061–1083 (2004).
2. L. Radziemski and D. Cremers, "A brief history of laser-induced breakdown spectroscopy; from the concept of atoms to LIBS 2012," *Spectrochim. Acta Part B* **87**, 3–10 (2013).
3. D. W. Hahn and N. Omenetto, "Laser-induced breakdown spectroscopy (LIBS), Part 1: review of basic diagnostics and plasma-particle interaction; still challenging issues within the analytical plasma community," *Appl. Spectrosc.* **64**, 335A–366A (2010).
4. D. W. Hahn and N. Omenetto, "Laser-induced breakdown spectroscopy (LIBS), Part II: review of instrumental and methodological approaches to material analysis applications to different fields," *Appl. Spectrosc.* **66**, 347–419 (2012).
5. F. J. Fortes and J. J. Laserna, "The development of fieldable laser-induced breakdown spectrometer; no limits on the horizon," *Spectrochim. Acta Part B* **65**, 975–990 (2010).
6. K. H. Kurniawan, M. O. Tjia, and K. Kagawa, "Review of laser-induced plasma, its mechanism and application to quantitative analysis of hydrogen and deuterium," *Appl. Spectrosc. Rev.* **49**, 323–434 (2014).
7. V. Lazic and S. Jovicevic, "Laser induced breakdown spectroscopy inside liquids: processes and analytical aspects," *Spectrochim. Acta Part B* **101**, 288–311 (2014).
8. T. Samu Jarvinen, S. Saari, J. Keskinen, and J. Toivone, "Detection of Ni, Pb and Zn in water using electrodynamic single-particle levitation and laser-induced breakdown spectroscopy," *Spectrochim. Acta Part B* **99**, 9–14 (2014).
9. M. Pardede, H. Kurniawan, M. O. Tjia, K. Ikezawa, T. Maruyama, and K. Kagawa, "Spectrochemical analysis of metal elements electrodeposited from water samples by laser-induced shock wave plasma spectroscopy," *Appl. Spectrosc.* **55**, 1229–1236 (2001).
10. R. Hedwig, W. Setia Budi, S. N. Abdulmajid, M. Pardede, M. M. Suliyanti, T. J. Lie, D. P. Kurniawan, K. H. Kurniawan, K. Kagawa, and M. O. Tjia, "Film analysis employing subtarget effect using 355 nm Nd-YAG laser-induced plasma at low pressures," *Spectrochim. Acta. Part B* **61**, 1285–1293 (2006).